Unexpected differences in the surface electronic structure of NiO and CoO observed by STM and explained by first-principles theory

M. R. Castell, S. L. Dudarev, G. A. D. Briggs, and A. P. Sutton

Department of Materials, University of Oxford, Parks Road, Oxford OX1 3PH, United Kingdom

Atomically resolved elevated-temperature scanning tunneling microscope (STM) images of (001) cobalt and nickel monoxide surfaces obtained under similar conditions show an order of magnitude difference in the atomic corrugation heights. Surface-electronic structure calculations taking into account the Hubbard U term show that on the CoO (001) surface the lowest unoccupied state has d_{xy} character as compared with the predominantly $d_{3z^2-r^2}$ lowest empty state on NiO (001). The difference in the symmetry of unoccupied d orbitals on CoO (001) and NiO (001) surfaces is responsible for the much lower level of atomic contrast observed in the STM images of cobalt oxide. [S0163-1829(99)04111-9]

In 1937, de Boer and Verwey[1] drew attention to a class of anomalous insulating transition-metal oxides, whose electronic structure could not be described using conventional band theory. De Boer and Verwey suggested that NiO might be considered as a prototype of this class of compounds noting at the same time that there was no great difference in the behavior of CoO and NiO. The origin of the insulating behavior of NiO and CoO was explained by Peierls and Mott[2] who pointed out that band theory may fail when the intersite tunnelling of electrons is suppressed by the Coulomb on-site repulsion between electrons. Subsequent studies of NiO and CoO were often performed in parallel[3,4] so that Brandow[5] referred to these oxides as the two most extensively studied Mott insulator materials.

Although at present a fully self-consistent approach to the calculation of the electronic structure of NiO and CoO still remains to be developed,[6] analysis of x-ray photoelectron spectra[7] show that both NiO and CoO belong to the class of charge-transfer insulators where the band gap separates filled oxygen $2p$ and empty metal $3d$ bands. The physical properties of CoO and NiO are very similar[8] with both oxides adopting the rocksalt crystal structure with lattice constants of 4.25 and 4.17 Å, respectively. The electronic structure of CoO and NiO is characterized by the $3d$ (Ref. 7) state of Co and the $3d$ (Ref. 8) state of Ni ions with the two $4s$ electrons transferred from metal to oxygen sites. In the octahedral field of oxygen ions the manifold of d states splits into e_g and t_{2g} subbands,[5] leading to the insulating ground state in the case of NiO.[9] In CoO the metal ions have one electron less per site, and this leads to the long debated[10] ambiguity in the population of the t_{2g} electronic orbitals and to the $\frac{2}{3}$ filled t_{2g} band. The incorrect prediction of a metallic ground state for CoO (Ref. 9) is the most striking example of the failure of conventional band theory.[6]

Another area where the properties of NiO and CoO were intensively investigated is the field of heterogeneous catalysis[12] where a considerable amount of information on surface d-shell excitations was accumulated by using electron-energy-loss spectroscopy,[13,14] and more recently by scanning tunneling microscopy (STM).[15–17] However, progress in understanding the STM images has been slow in

contrast with rapid advances in the interpretation of metallic[18,19] and band-insulating systems[20] where images were successfully analyzed on the basis of *ab initio* density-functional calculations.

In this paper we describe results of a comparative STM experimental and *ab initio* theoretical study carried out for Mott insulating CoO and NiO (001) (1×1) surfaces. We show atomically-resolved STM images of the unreconstructed CoO (001) surface and compare the atomic corrugation heights with data from images of the NiO (001) surface.[22] The STM results are interpreted using electronic structure calculations performed using a method combining the local spin-density approximation (LSDA) of the density-functional theory with the Hubbard U term (LSDA+U). We show that this analysis makes it possible not only to explain the origin of the observed large difference in the contrast of STM images of NiO and CoO surfaces, but also to obtain evidence for the type of ordering of d orbitals in the Ni and Co ions situated in the surface atomic layer.

The experiments were carried out in a JEOL JSTM-4500XT elevated temperature STM on single crystals of black CoO and black NiO (Ref. 21) using etched Pt/Ir or W tips. Samples of CoO and NiO were cleaved under UHV conditions (2×10^{-8} Pa) to reveal (001) surfaces and imaged in the STM at elevated temperatures. At room temperature the sample resistivity was too high to be easily measured for the CoO crystal (literature value 10^8 Ω cm) and measured to be 100 Ω cm for the Li-doped NiO crystal. At the imaging temperature of 200 °C the electrical resistivities decreased to 10^5 Ω cm and 10 Ω cm for the CoO and NiO samples, respectively. These lowered resistivities at elevated temperature substantially assisted successful STM imaging.

STM images of the (001) cleavage surfaces of both CoO and NiO reveal atomically flat terraces separated by monatomic steps that run in $\langle 001 \rangle$ directions. The terraces generally have a low defect density and are arranged in the bulk-terminated (1×1) structure as determined by STM and low-energy electron diffraction.[11] NiO cleaves slightly more easily than CoO, which is evident by the terrace structure of the cleavage surfaces. In NiO terrace widths between $\langle 001 \rangle$
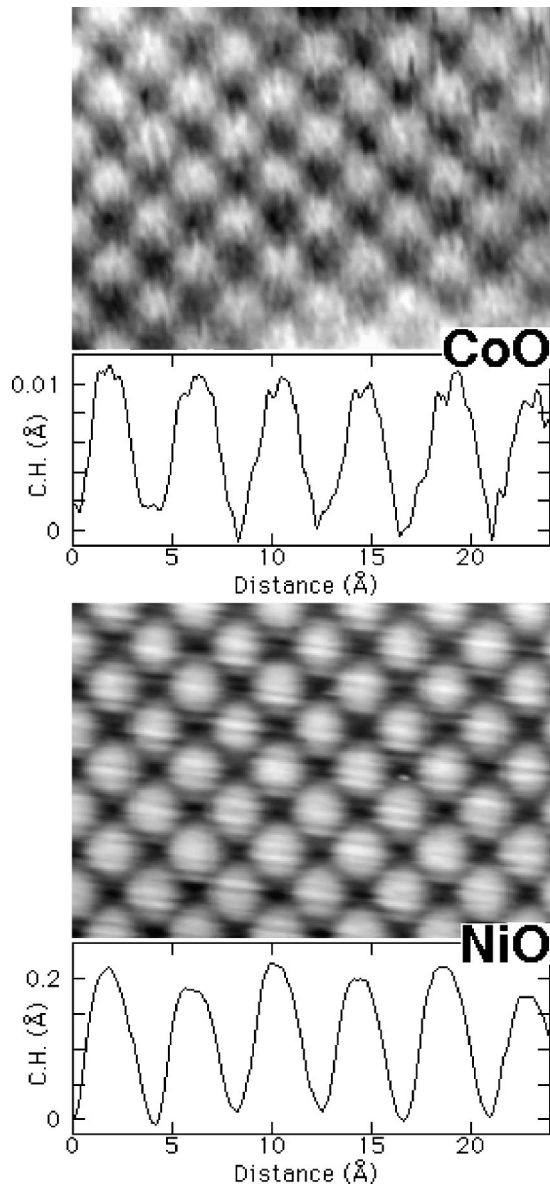
FIG. 1. Empty states STM images of CoO (top), (V_{sample} $= 2.7V$, $I_{\text{tunnel}} = 0.57$ nA), and NiO (bottom), (V_{sample} $= 1.3V$, $I_{\text{tunnel}} = 1.0$ nA), (001) (1×1) UHV cleavage surfaces, where the bright dots show the Co and Ni ions, respectively. Corrugation heights (CH) are shown as horizontal line scans taken through the center of the images. The CoO image (top) was taken in constant height mode and the corresponding calculated 0.01 Å height corrugations are shown below the image. These can be compared with the order of magnitude larger 0.2 Å corrugations observed directly using the constant current mode for the NiO sample. Image widths are 24 Å.

steps are between 10 and 50 nm, whereas for CoO the terrace widths are generally smaller and lie between 5 and 30 nm. Empty states STM images of the (1×1) termination of the (001) UHV cleavage surfaces for both oxides are shown in Fig. 1. While the atomically resolved images of CoO and NiO look similar, there is a significant difference in the atomic corrugation heights as indicated by the vertical scales of the line scans in each case. The NiO image was taken using the familiar constant current mode where the corrugation heights can be measured directly because the tip follows

the contours of a constant probability tunneling surface. All the NiO atomic resolution images analyzed show corrugation heights of 0.15 to 0.2 Å, which tend to be at a maximum at sample biases around 1.5 V. However, when imaging the CoO (001) (1×1) surface in the constant current mode no atomic resolution images can be obtained and the surface appears flat within the noise limit. We found that it is necessary to use the more sensitive constant height mode, where changes in the tunneling current are mapped and the tip is held at a constant height, to obtain the kind of atomic resolution images shown in Fig. 1 (top). Atomic resolution for the (1×1) surface of CoO (001) was found to be possible at sample biases of around 3 V. Biases significantly below this value resulted in repeated tip crashes, and biases much above 3 V did not allow atomic resolution imaging but were well suited to trace sample topography. The CoO corrugations in Fig. 1 represent a change of 2% in the tunnelling current between the peaks and the troughs, which corresponds to a calculated corrugation height[26] of around 0.01 Å and is an order of magnitude lower than for the NiO sample. A direct comparison between the sample bias and the position of the empty states relative to the Fermi level was not possible due to the unknown positions of the Fermi levels of our samples as well as effects such as band bending and possibly a voltage drop across a non-Ohmic contact. However, we are confident that the STM images in Fig. 1 are created from tunneling into empty surface states near the bottom of the conduction band because the sample biases used for imaging were around 0.1 V higher that those that regularly resulted in tip crashes. This also indicates that the tip-sample separations were at comparable distances for the CoO and NiO images shown in Fig. 1. The different conductivities of the samples are unlikely to affect the corrugation heights, as previous STM experiments on Si surfaces have shown that the contrast of empty states images is independent of the dopant level.[27] Numerous attempts were made to obtain atomically resolved filled states STM images of the CoO (001) surface so that the corrugation heights could be compared with the filled states images obtained of NiO (001). However, we were not able to image the filled states on CoO (001).

Given that the majority of physical properties of NiO and CoO are very similar,[8] the surprisingly large observed difference in the corrugation heights of the STM images requires an explanation. Since LSDA fails to describe the electronic structure of Mott insulating compounds,[9,23,24] the density functional approaches that were successfully applied to the interpretation of STM images of metallic and band insulating systems[18–20] are unsuitable for interpreting the STM images of NiO and CoO surfaces. LSDA calculations predict band gaps that are either too small (NiO) or nonexistent (CoO),[9] and this is at odds with the observed high electrical resistivity of these oxides. To describe the effect of strong correlations between electrons in d shells of metal ions on the electronic structure of NiO and CoO surfaces, we used a modified density-functional approach combining the LSDA description of delocalized electronic orbitals with a Hubbard U term included for localized d states (LSDA$+U$).[25,28] Calculations were carried out for antiferromagnetically ordered 12-atom slabs of NiO and CoO. For both cases, we used 18 k points in the full (1×1) surface Brillouin zone and the same values of the Hubbard $\bar{U}$ and the exchange integral $\bar{J}$ as
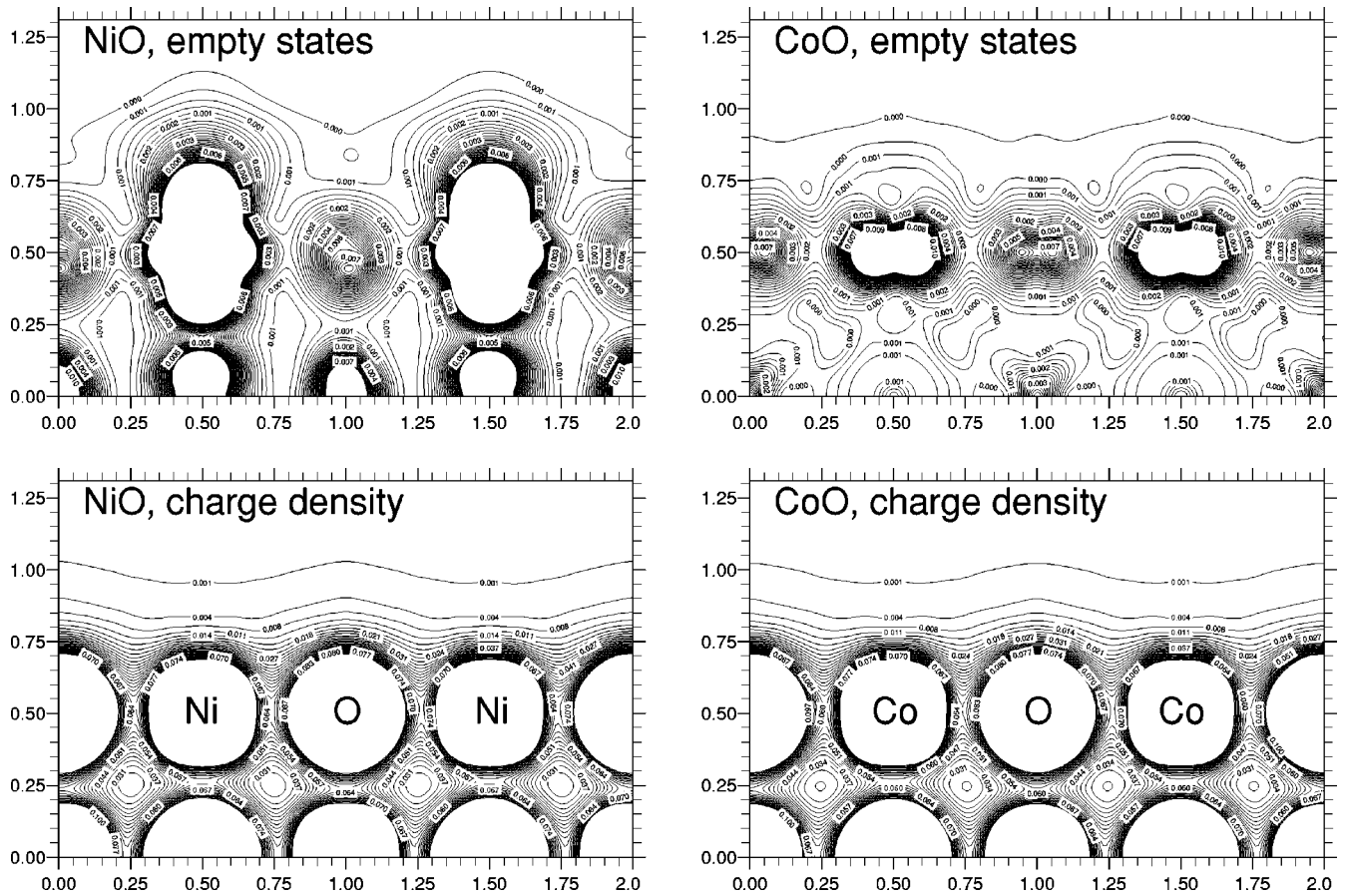
FIG. 2. Bottom: valence electron charge-density distributions calculated numerically for NiO and CoO (001) antiferromagnetically ordered surfaces. Top: the distribution of the density of empty states calculated for the same surfaces by summing over a 1-eV interval corresponding to the bottom of the conduction band. Figures in boxes represent values of charge density in atomic units. Distances parallel and normal to the surface are expressed in units of the respective lattice constant.

we obtained from an analysis of the total energy and electron-energy-loss spectra in Ref. 28. The assumed bulk-terminated crystal structure is consistent with experimental data showing less than 2% surface relaxation.[29] Following the approach developed in Ref. 20, to interpret STM images obtained at a positive sample bias we investigated the asymptotics of the real-space distribution of the density of unoccupied electronic states summed over a 1 eV interval of energies above the conduction-band minimum.

At each cation site of bulk NiO the majority spin d states are fully occupied while, for the minority spin, the t_{2g} states are filled and the e_g states are empty.[5,9] On the (001) surface of NiO the crystal field of five neighboring anions has an almost negligible effect on the occupancies of the d states. CoO poses a somewhat more difficult problem because only two out of three t_{2g} minority spin states are occupied, and the ordering of t_{2g} states is determined by weak effects, namely spin-orbit coupling and Jahn-Teller distortion.[5,9] Since all the experimental STM images of CoO surfaces were obtained at temperatures significantly higher than the Neél temperature, $T_N = 290$ K, where no lattice distortion was present,[8] the proper linear combinations of t_{2g} states were determined by spin-orbit interactions. LSDA+U total energy calculations showed that for bulk CoO the configuration with the $Y_{2,-1} = (d_{zx} - i d_{yz})/\sqrt{2}$ minority spin state empty and d_{xy} and $Y_{2,1}$ minority spin states filled on each Co

ion, was approximately 0.2 eV/(primitive unit cell) lower than the alternative configuration[25] with minority spin d_{xy} state empty and d_{zx} and d_{yz} states occupied. The magnetic moment of a Co ion evaluated for the first configuration was found to be $\sim 3.7 \mu_B$ ($m_{spin} = 2.64 \mu_B$ plus $m_{orb} = 1.06 \mu_B$) in agreement with the experimental value of $3.8 \mu_B$ observed for bulk specimens.[30] The orbital contribution to the magnetic moment for the second configuration $m_{orb} = 0.75 \times 10^{-2} \mu_B$ is considerably smaller than the value observed experimentally.[30] It is therefore the first of the two above configurations that represents the ground state of *bulk* CoO. Our surface-electronic structure calculations revealed that in the lowest total energy state the Co ions in the surface layer adopt the minority spin d_{xy}-empty/d_{zx} and d_{yz}-filled configuration while the subsurface layer retains the bulk $Y_{2,-1}$-empty/d_{xy} and $Y_{2,1}$-filled ordering pattern. For cobalt ions in the surface atomic layer the energy of the d_{xy} orbital is approximately $0.86 e^2 \langle r^2 \rangle / a^3$ higher than energies of either d_{zx} or d_{yz} states, where $\langle r^2 \rangle$ is the mean-square radius of the d shell and a is the distance between the centers of the Co and O ions. No orbital contribution to the magnetic moment is therefore present for Co ions in the surface layer.

The observed difference in the contrast of STM images of NiO and CoO (001) surfaces can now be explained by examining distributions of the density of empty states integrated over an interval of energies above the conduction-

band minimum.[20] The similarity between *charge-density* distributions shown in Fig. 2 reflects the similarity of the physical properties of the two oxides.[8] But the distributions of the densities of *unoccupied* states shown in Fig. 2 are dissimilar, the CoO (001) surface showing smaller corrugations than the NiO (001) surface. The nature of this effect is associated with the difference in the shape of the $d_{3z^2-r^2}$ and d_{xy} orbitals representing the lowest-lying unoccupied electronic states on NiO (001) and CoO (001) surfaces, respectively. For comparison, we note that if the bulk ordering of t_{2g} states were retained for Co ions in the surface layer, the STM image contrast would be predicted to be similar to that obtained for the NiO surface, and this would conflict with our experimental observations. We may therefore conclude that the STM observations allow us to distinguish between two possible types of ordering of t_{2g} states on the CoO (001) surface. The type of ordering consistent with the observed low level of image contrast is associated with a negligible orbital contribution to the magnetic moment of Co ions in the surface layer. This prediction could be verified by measuring the magnetic moment of surface Co ions using spin-polarized low-energy electron diffraction.[31]

In summary, we have reported the first atomically-resolved STM observations of unreconstructed (1×1) CoO (001) surfaces and compared them with STM images of NiO (001). The difference in symmetry of the lowest unoccupied d states on CoO (001) and NiO (001) predicted by our *ab initio* LSDA+U calculations explains the observed large difference in the atomic corrugation heights seen in our STM images.

[1] J. H. de Boer and E. J. W. Verwey, Proc. Phys. Soc. London **49**, 59 (1937).

[2] R. Peierls, communicated by N. F. Mott, see J. H. de Boer and E. J. W. Verwey, Proc. Phys. Soc. London **49**, 72 (1937).

[3] R. J. Powell and W. E. Spicer, Phys. Rev. B **6**, 2182 (1970).

[4] Z.-X. Shen, C. K. Shih, O. Jepsen, W. E. Spicer, I. Lindau, and J. W. Allen, Phys. Rev. Lett. **64**, 2442 (1990).

[5] B. H. Brandow, Adv. Phys. **26**, 651 (1977).

[6] P. Fulde, *Electron Correlations in Molecules and Solids*, 3rd ed. (Springer, Berlin, 1995).

[7] J. Zaanen and G. A. Sawatzky, Prog. Theor. Phys. Suppl. **101**, 231 (1990).

[8] V. S. Mandel, J. Cryst. Growth **174**, 346 (1997).

[9] K. Terakura, A. R. Williams, T. Oguchi, and J. Kübler, Phys. Rev. Lett. **52**, 1830 (1984).

[10] M. R. Norman, Phys. Rev. Lett. **64**, 1162 (1990).

[11] M. Prutton, J. A. Walker, M. R. Welton-Cook, R. C. Felton, and J. A. Ramsey, Surf. Sci. **89**, 95 (1979).

[12] V. E. Henrich and P. A. Cox, *The Surface Science of Metal Oxides* (Cambridge University Press, Cambridge, 1994).

[13] A. Freitag, V. Staemmler, D. Cappus, C. A. Ventrice, K. Al Shamery, H. Kuhlenbeck, and H.-J. Freund, Chem. Phys. Lett. **210**, 10 (1993).

[14] B. Fromme, M. Möller, Th. Anschütz, C. Bethke, and E. Kisker, Phys. Rev. Lett. **77**, 1548 (1996).

[15] T. Bertrams and H. Neddermeyer, J. Vac. Sci. Technol. B **14**, 1141 (1996).

[16] H. J. Freund, B. Dillmann, O. Seiferth, G. Klivenyi, M. Bender, D. Ehrlich, I. Hemmerich, and D. Cappus, Catal. Today **32**, 1 (1996).

[17] S. Weichel and P. J. Møller, Surf. Sci. **399**, 219 (1998).

[18] J. A. Stroscio, D. T. Pierce, A. Davies, R. J. Celotta, and M. Weinert, Phys. Rev. Lett. **75**, 2960 (1995).

[19] A. Biedermann, O. Genser, W. Hebenstreit, M. Schmid, J. Redinger, R. Podloucky, and P. Varga, Phys. Rev. Lett. **76**, 4179 (1996).

[20] U. Diebold, J. F. Anderson, K.-O. Ng, and D. Vanderbilt, Phys. Rev. Lett. **77**, 1322 (1996).

[21] The CoO crystal was grown by Crystal GmbH, Germany. The NiO crystal was grown by K & R Creations, Japan. Trace element analysis of these samples was carried out using a scanning proton microprobe, which revealed that the dominant impurity was Fe at a concentration of 0.12% by weight in CoO and at a concentration of 0.09% by weight in NiO. The NiO crystal also contained Li, which was introduced purposefully as a dopant to decrease the electrical resistivity and was measured at 0.016% by weight.

[22] M. R. Castell, P. L. Wincott, and N. G. Condon *et al.*, Phys. Rev. B **55**, 7859 (1997).

[23] F. Manghi, C. Calandra, and S. Ossicini, Phys. Rev. Lett. **73**, 3129 (1994).

[24] F. Aryasetiawan and O. Gunnarsson, Phys. Rev. Lett. **74**, 3221 (1995).

[25] V. I. Anisimov, J. Zaanen, and O. K. Andersen, Phys. Rev. B **44**, 943 (1991); V. I. Anisimov, F. Aryasetiawan, and A. I. Lichtenstein, J. Phys.: Condens. Matter **9**, 767 (1997).

[26] The tunneling conductance σ is related to the tip-sample separation distance d through $\sigma \sim \exp(-2kd)$, see J. Tersoff and D. D. Hamann, Phys. Rev. Lett. **50**, 1998 (1993). Assuming 4 eV for the work function, we obtain $k \sim 1.02$ Å^{-1}. The maximum amplitude of the corrugations $d_{max} - d_{min}$ is given by $(2k)^{-1}\ln(I_{max}/I_{min}) \approx 0.01$ Å for the measured ratio $I_{max}/I_{min} \approx 1.019$.

[27] J. Tersoff and D. R. Hamann, Phys. Rev. B **31**, 805 (1985).

[28] S. L. Dudarev, G. A. Botton, S. Y. Savrasov, C. J. Humphreys, and A. P. Sutton, Phys. Rev. B **57**, 1505 (1998); S. L. Dudarev, G. A. Botton, S. Y. Savrasov, D. Szotek, W. M. Temmerman, and A. P. Sutton, Phys. Status Solidi A **166**, 429 (1998).

[29] F. P. Netzer and M. Prutton, J. Phys. C **8**, 2401 (1975).

[30] D. Herrmann-Ronzaud, P. Burlet, and J. Rossat-Mignot, J. Phys. C **11**, 2123 (1978).

[31] H. Tang, M. Plihal, and D. L. Mills, Phys. Rev. B **54**, 14 172 (1996).